

锅炉水冷壁管在含 SO_4^{2-} 溶液中的点蚀特性研究

熊书华 朱志平 荆玲玲 张 辉

(长沙理工大学 化学与生物工程学院 湖南 长沙 410076)

摘 要: 为研究水冷壁管材料 15CrMo 在含 SO_4^{2-} 溶液中的点蚀特性,通过常温电化学实验和高温挂片实验,对常温性能和高温腐蚀特性进行分析,用透反射金像显微镜、SEM、EDS、XRD 对试片表面形态和组分进行表征与分析。结果表明:常温条件下, SO_4^{2-} 主要以氧化作用为主,抑制不锈钢的腐蚀,材料的耐蚀性增加;高温条件下, SO_4^{2-} 为侵蚀性离子,将加速材料的点蚀,形成带有锯齿状边缘的点蚀坑,其点蚀临界浓度为 1mg/L;常温下 SO_4^{2-} 抑制 Cl^- 点蚀的机理是竞争吸附,高温条件下 SO_4^{2-} 促进点蚀的机理为局部酸化理论。

关 键 词: 水冷壁管; 15CrMo; SO_4^{2-} ; 点蚀

中图分类号: TK 224. 9 文献标识码: A

引 言

随着机组参数的增加,锅炉热负荷的升高,对锅炉给水品质的要求越来越严格^[1-3]。如果给水中杂质离子含量超过允许浓度,将加速锅炉的结垢和腐蚀,引起炉管水侧腐蚀,严重时导致爆管^[4],在实际生产过程中, SO_4^{2-} 对管材的影响已经引起人们的关注^[5-6]。

虽然对锅炉烟气侧水冷壁管的腐蚀、高温气体中水冷壁高温氧化的机理、侵蚀性离子 Cl^- 的影响等方面已经进行了大量的研究^[7-11],但是针对水冷壁管在含有 SO_4^{2-} 离子的锅水中的研究则不多见。本研究对锅炉水冷壁材料 15CrMo 进行常温电化学实验和高温挂片实验,用透反射金像显微镜、扫描电

子显微镜 (SEM)、能谱仪 (EDS)、X 射线衍射仪 (XRD) 进行试片表面形态和组分的表征与分析,得出该材料在常温和高温条件下的腐蚀特性,为锅炉中 SO_4^{2-} 的控制提供理论依据。

1 实验内容

1.1 主要仪器及试剂

GCF 永磁旋转搅拌式反应釜; CHI660C 电化学工作站; 日本理学 D/max - 2500/PC 型 X 射线衍射仪; 扫描电子显微镜(含 EDS 能谱仪) (Quanta200, 荷兰 FEI); 透反射金相显微镜; 岛津原子吸收分光光度计; 岛津 AUY120 型电子天平; Na_3PO_4 , NaOH , NaCl , Na_2SO_4 (分析纯); 去离子水。

1.2 试片处理

选用 1 000 MW 机组水冷壁管作为实验材料,其化学成份如表 1 所示。将管材加工成 1 cm × 1 cm 的正方形试片,工作面背面焊上铜导线,用环氧树脂封装非工作面,作常温电化学实验用工作电极。高温实验用试片规格为 40 mm × 12 mm × 2 mm。实验前依次用 200、400、600 和 1 000 目砂纸对工作电极和试片进行打磨,更换砂纸时改变打磨方向 90°,每次都打磨掉前一次的痕迹。打磨完后擦去污物,然后用酒精、丙酮分别清洗,去除油脂,冷风吹干,再用滤纸包好放置干燥器中一定时间后称重备用。

表 1 水冷壁管材料的主要成份

Tab. 1 Main constituents of the waterwall tube material

	化学成份 / %									
	C	Si	Mn	P	S	Cr	Mo	Cu	Ni	V
15CrMo	0.12 ~ 0.18	0.12 ~ 0.18	0.17 ~ 0.37	0.4 ~ 0.7	≤0.03	≤0.03	0.8 ~ 1.1	0.40 ~ 0.55	≤0.2	≤0.3

1.3 实验方法

实验介质为实验室配置的模拟低磷酸盐-低

NaOH 水工况锅水,组成为: $\text{PO}_4^{3-} \leq 2.5 \text{ mg/L}$, Na^+

收稿日期: 2011 - 01 - 25; 修订日期: 2011 - 03 - 05

基金项目: 湖南省自然科学基金资助项目 (09JJ6067)、湖南省科技攻关项目基金资助 (2010GK3171)

作者简介: 熊书华 (1986 -), 女, 湖南湘乡人, 长沙理工大学硕士研究生。

$\leq 0.85 \text{ mg/L}$, $\text{Cl}^- \leq 0.028 \text{ mg/L}$, $\text{SO}_4^{2-} \leq 0.028 \text{ mg/L}$, $\text{SiO}_2 \leq 0.2 \text{ mg/L}$, $\text{pH} = 9.5 \pm 0.5$ 。

电化学实验在 CHI660C 电化学工作站上进行,测定时采用饱和甘汞电极为参比电极,铂电极为辅助电极。Tafel 曲线扫描速度 2 mV/s 。实验前充 40 min 氮气,以除去水中的溶解氧。

高温实验在容积为 1 L 的高压釜中进行。首先将配置好的 600 mL 模拟锅水倒入洁净的高压釜中,用镍铬丝将处理好的试片悬挂于高压釜的液相中,充 40 min 氮气,缓慢将温度升至 $300 \text{ }^\circ\text{C}$,恒温 7 h 后冷却至室温,将试片取出,依次用去离子水、酒精、丙酮清洗,冷风吹干。观察并记录表面的腐蚀情况,放入干燥器中,放置与预处理相同的时间后称重,并进行表面形貌分析和成份分析,锅水中的铁离子浓度用原子吸收分光光度计进行测定。

试片的腐蚀速率用增重法进行计算:

$$v = \Delta m / A \cdot t \quad (1)$$

式中: Δm —实验后试片重量的变化; A —试片的表面积; t —实验时间。

为避免 SO_4^{2-} 吸附在高压釜内衬上而干扰实验,高压釜在每次实验前都要用 NaOH 浸泡,然后用去离子水反复冲洗,直至出水的电导率与去离子水的电导率一致。

2 结果与讨论

2.1 SO_4^{2-} 对试片的电化学性能影响

常温下测试工作电极在含不同浓度 SO_4^{2-} 的模拟低磷酸盐-低 NaOH 水工况溶液中获得极化曲线如图 1 所示。

由图 1(a) 可见, SO_4^{2-} 浓度较低时,极化曲线变化不大,溶液中 SO_4^{2-} 达到一定浓度后,工作电极的腐蚀电位随着 SO_4^{2-} 浓度的增加而逐渐升高,耐点蚀性能增强。对极化曲线进行分析可以得出相关的电化学参数,如表 2 所示。随着 SO_4^{2-} 浓度的增加,腐蚀电流 (I_{corr}) 降低,腐蚀速度降低,腐蚀电位 (E_{corr}) 升高,这说明 SO_4^{2-} 有抑制点蚀的作用。

Cl^- 浓度为 10 mg/L ,随着 SO_4^{2-} 浓度变化的极化曲线如图 1(b)。随着 SO_4^{2-} 浓度增加, E_{corr} 升高, I_{corr} 降低。这是由于 SO_4^{2-} 为含氧酸,有一定的钝化性能,当溶液中的 SO_4^{2-} 增加时,其与 Cl^- 之间存在竞争吸附的作用,使得电极表面有效吸附的 Cl^- 浓度降低,所以电极的耐蚀性增加。

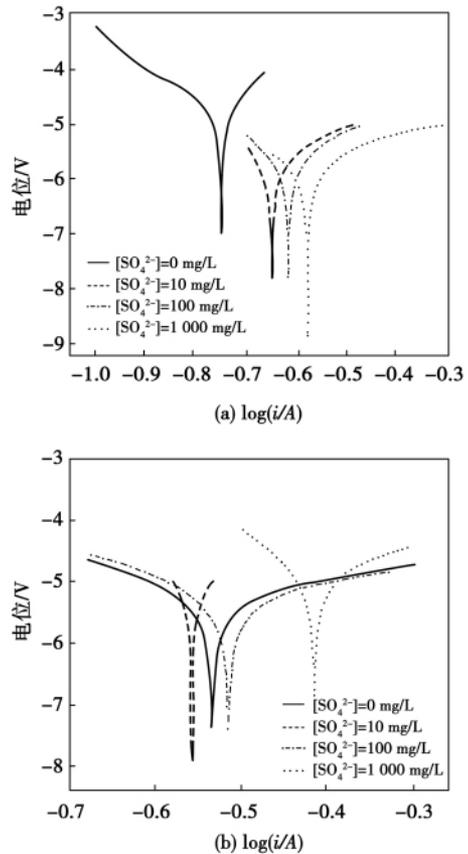


图 1 SO_4^{2-} 对塔菲尔曲线的影响

Fig. 1 Influence of SO_4^{2-} on Tafel curves

表 2 SO_4^{2-} 对试片的电化学参数的影响

Tab. 2 Influence of SO_4^{2-} on electrochemical parameters of the test piece

$[\text{Cl}^-] / \text{mg} \cdot \text{L}^{-1}$	$[\text{SO}_4^{2-}] / \text{mg} \cdot \text{L}^{-1}$	$E_{\text{corr}} / \text{V}$	$I_{\text{corr}} / \text{A}$
0	0	-0.752	1.919×10^{-5}
	10	-0.653	9.977×10^{-7}
	100	-0.620	6.99×10^{-7}
	1000	-0.592	5.8×10^{-7}
10	0	-0.563	9.994×10^{-6}
	10	-0.559	9.885×10^{-6}
	100	-0.536	5.314×10^{-6}
	1000	-0.418	4.908×10^{-6}

2.2 SO_4^{2-} 对试片的高温性能影响

从图 2(a) 中可以看出, $C_{\text{SO}_4^{2-}} < 5 \text{ mg/L}$ 时,增重速率为正,这是由于 SO_4^{2-} 浓度较低,溶液中的阴离子主要为 OH^- ,试片表面发生氧化,而且 SO_4^{2-} 为含氧酸,也有一定的氧化作用,此时是以氧化速率为

主。当 $C_{\text{SO}_4^{2-}} > 5 \text{ mg/L}$ 时, SO_4^{2-} 对材料的侵蚀作用大于氧化作用, 增重速率开始下降, 甚至为负数。这时, 试片的溶解速率大于试片的氧化速率, 溶液中 Fe 浓度增加。经数据拟合可以得出, 溶液中 Fe 浓度与 SO_4^{2-} 浓度呈对数函数关系:

$$C_{\text{Fe}} = 0.121 + 0.04 \ln(C_{\text{SO}_4^{2-}})$$

当溶液中 Cl^- 浓度为 0.8 mg/L 时, 随着 SO_4^{2-} 浓度增加, 腐蚀速率的变化曲线如图 2 (b) 所示。当 SO_4^{2-} 浓度较低时, 试片的腐蚀速率变化不大, 随着 SO_4^{2-} 浓度增加, 试片溶解速率显著增加, 这说明高温条件下 SO_4^{2-} 是侵蚀性离子, Fe 浓度与 $\text{Cl}^- / \text{SO}_4^{2-}$ 呈对数函数关系:

$$C_{\text{Fe}^{2+}} = 1.331 + 0.48 \ln(C_{\text{Cl}^-} / C_{\text{SO}_4^{2-}})$$

图 3 为不同 SO_4^{2-} 浓度下高温实验试片的透反射金相显微镜图谱。从图中可以看出, SO_4^{2-} 为 0.4 mg/L 时, 试片表面无点蚀, 与空白时的试片相似, 当 SO_4^{2-} 为 1 mg/L 时, 试片表面出现黑点, 随着 SO_4^{2-} 浓度增加, 点蚀越来越明显, 并出现锯齿状的边缘。这也说明高温下 SO_4^{2-} 会导致点蚀的发生, 其临界浓度为 1 mg/L 。

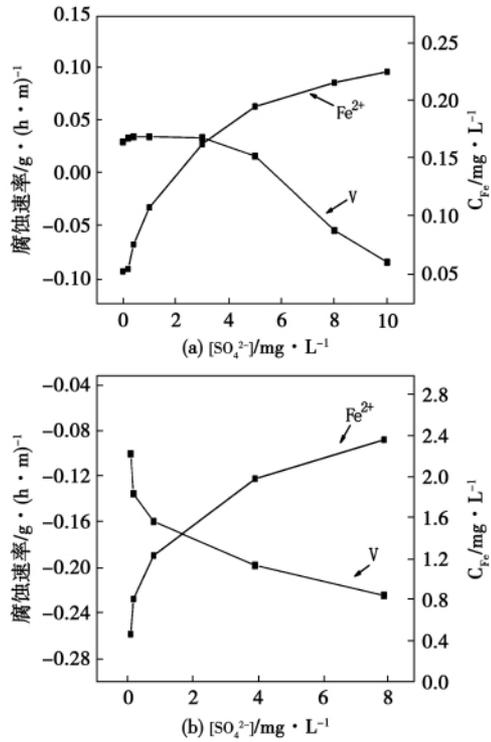
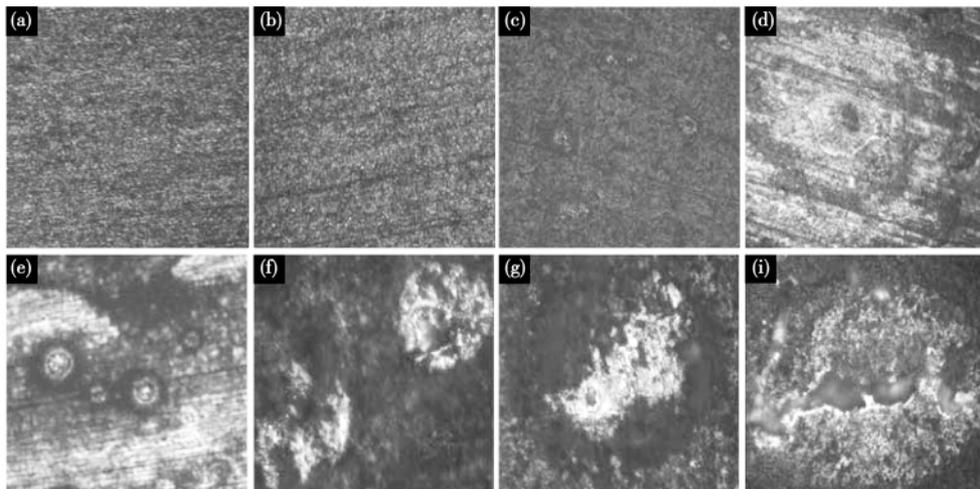


图 2 SO_4^{2-} 对高温腐蚀速率的影响
Fig. 2 Influence of SO_4^{2-} on the corrosion rate at a high temperature



(a) $[\text{SO}_4^{2-}] = 0 \text{ mg/L}$; (b) $[\text{SO}_4^{2-}] = 0.4 \text{ mg/L}$; (c) $[\text{SO}_4^{2-}] = 1 \text{ mg/L}$; (d) $[\text{SO}_4^{2-}] = 3 \text{ mg/L}$; (e) $[\text{SO}_4^{2-}] = 5 \text{ mg/L}$;
(f) $[\text{SO}_4^{2-}] = 8 \text{ mg/L}$; (g) $[\text{SO}_4^{2-}] = 10 \text{ mg/L}$; (h) $[\text{SO}_4^{2-}] = 15 \text{ mg/L}$

图 3 高温实验试片的透反射金相显微镜图

Fig. 3 Pictures of the test piece at a high temperature photographed by using a lens reflection-based metallogenic microscope

2.3 SEM 和 XRD 分析

SO_4^{2-} 浓度为 8 mg/L 时, 点蚀表面的形态如图 4 所示, 进行能谱分析得出其表面主要有 Cr、Mn、Fe、O 等。对高温试片进行断面电镜扫描和能谱分析,

如图 5 所示。氧化膜分为两层, 外层富含 Fe。对高温试片表面进行 XRD 分析如图 6 所示, 高温氧化膜主要成分为 Fe_3O_4 , 还有 Mn、Cr 氧化物等, 这与图 6 一致。

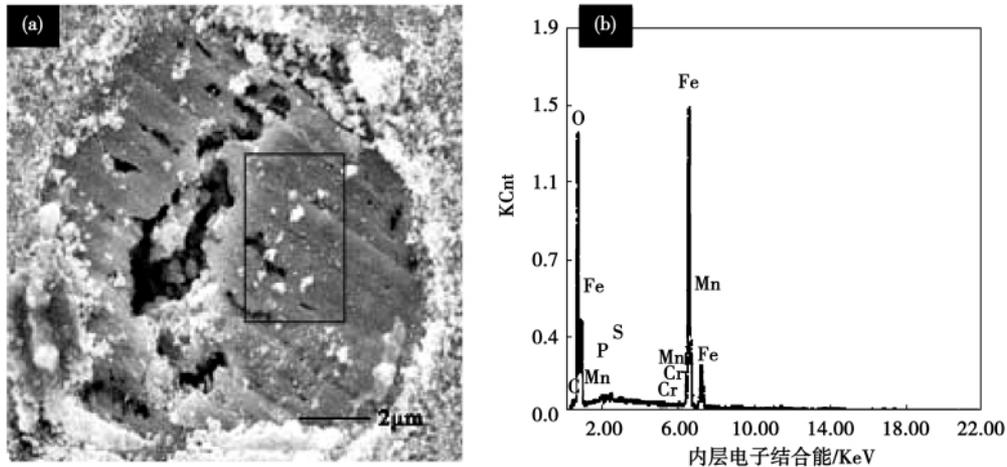


图 4 高温试片表面 SEM 及 EDS 图谱

Fig. 4 SEM and EDS atlas of the surface of the test piece at a high temperature

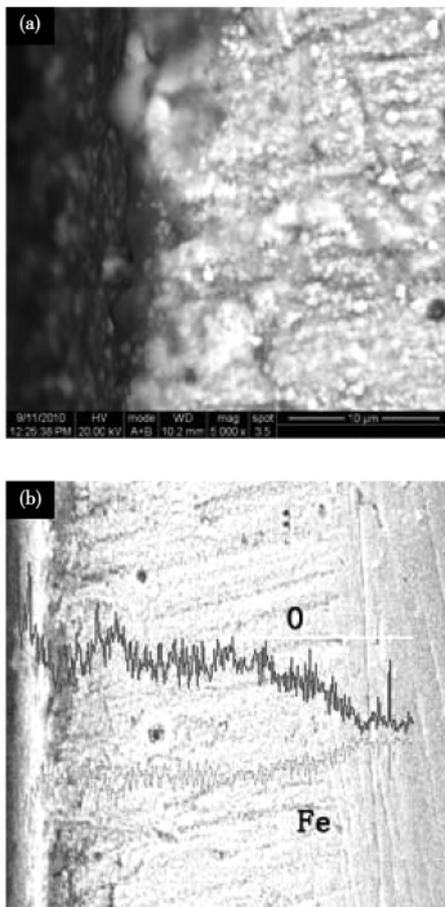
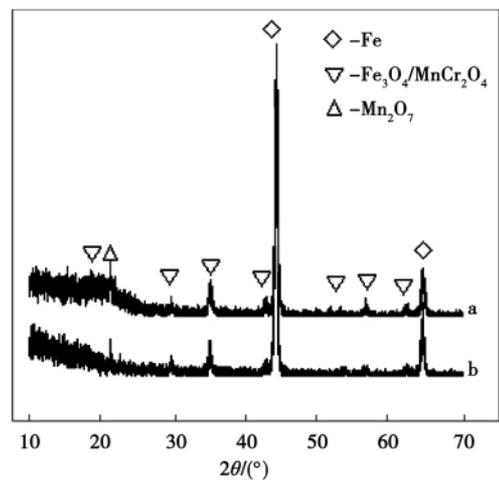


图 5 EDS 线扫描截面图谱

Fig. 5 EDS line-by-line scanned atlas of a section

由上可知 SO_4^{2-} 并不影响高温氧化膜的双层结构。但是随着溶液中 SO_4^{2-} 浓度增大, SO_4^{2-} 将吸附在试片表面, 在氧化膜表面形成一个静电场, 当

SO_4^{2-} 浓度增加到一定程度后, 该离子将与氧化膜中的阳离子结合, 如式 (2) 生成可溶的 $FeSO_4$, 结果在试片表面形成小蚀坑, 这些小蚀坑即为点蚀核。随着 SO_4^{2-} 浓度继续增加, $FeSO_4$ 将发生水解, 生成 H^+ , 如式 (3) 和 (4) 所示。 H^+ 在小蚀坑中浓缩, 试片表面形成局部酸化, 促使点蚀核生长成为蚀孔。蚀孔内为酸性环境, 基体金属处于活化状态, 将发生溶解, 阳极溶解反应如式 (5) 所示, 阴极反应为式 (6) 所示, 蚀孔将进一步发展, 腐蚀加剧。



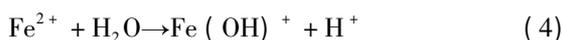
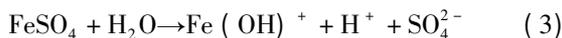
a $[Cl^-] = 0.8 \text{ mg/L}, [SO_4^{2-}] = 8 \text{ mg/L};$

b $[Cl^-] = 0 \text{ mg/L}, [SO_4^{2-}] = 8 \text{ mg/L}$

图 6 高温试片表面 XRD 图谱

Fig. 6 XRD atlas of the surface of the test piece at a high temperature





当水中的可溶性盐转化为沉淀物,沉积在蚀孔口时,将会形成一个闭塞电池。孔内金属硫酸盐进一步浓缩,其水解使得介质酸度继续增加,基体金属持续处于活化状态,蚀孔向纵深发展。

3 结 论

(1) 常温下,随着 SO_4^{2-} 浓度的增加, I_{corr} 降低, E_{corr} 升高, SO_4^{2-} 有缓蚀作用。

(2) 常温下 SO_4^{2-} 抑制 Cl^- 点蚀的机理是由于这两种离子在材料表面存在竞争吸附,使得电极表面有效吸附的 Cl^- 浓度降低,材料的耐蚀性增加。

(3) 高温条件下, SO_4^{2-} 为侵蚀性离子,促进材料的溶解,加速材料的点蚀,形成带有锯齿状边缘的点蚀坑, SO_4^{2-} 的临界浓度为 1 mg/L。

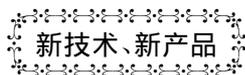
(4) 高温 SO_4^{2-} 促进点蚀的机理是由于 SO_4^{2-} 促进 Fe^{2+} 水解, H^+ 浓度增加,局部酸化,点蚀加剧。

参考文献:

- [1] 朱志平,孙本达,李宇春. 电站锅炉水化学工况及优化[M]. 北京: 中国电力出版社, 2009.
ZHU Zhi-ping, SUN Ben-da, LI Yu-chun. Water chemical condition and optimization of a utility boiler[M]. Beijing: China Electric Power Press, 2009.
- [2] Lucan Dumitra. Behaviour of the steam generator tubing in water with different pH values[J]. Nucl. Eng. Des, 2010, doi: 10.1016/j.nucengdes.2010.03.029.
- [3] 朱志平,黄可龙,张玲等. 高温状态下炉水 pH 值的变化特征研究[J]. 热能动力工程, 2005, 20(2): 182-185.
ZHU Zhi-ping, HUANG Ke-long, ZHANG Ling et al. Study of the PH value variation characteristics of water in a boiler at a high temperature[J]. Engineering for thermal energy and power, 2005, 20

- (2): 182-185.
- [4] 朱志平,黄可龙,杨道武等. 锅炉给水系统腐蚀原因分析[J]. 腐蚀科学与防护技术, 2005, 17(3): 195-197.
ZHU Zhi-ping, HUANG Ke-long, YANG Dao-wu et al. Analysis of the causes for corrosion in a boiler feedwater system[J]. Corrosion science and prevention technology, 2005, 17(3): 195-197.
- [5] 朱志平. 压水堆核电厂水化学工况及优化[M]. 北京: 原子能出版社, 2010.
ZHU Zhi-ping. Water chemical condition and optimization of a pressurized water reactor-based nuclear power plant[M]. Beijing: Atomic Energy Press, 2010.
- [6] 朱兴宝,熊京川,梁桥哄. 岭澳核电站二期凝结水处理系统重大技术改进[J]. 核动力工程, 2009, 30(6): 1-5.
ZHU Xing-bao, XIONG Jing-chuan, LIANG Qiao-hong. Major technical improvement in the condensate water treatment system in Phase II of Lingao Nuclear Power Station[J]. Nuclear Power Engineering, 2009, 30(6): 1-5.
- [7] 赵虹,魏勇. 燃煤锅炉水冷壁烟侧高温腐蚀的机理及影响因素[J]. 动力工程, 2002, 22(2): 1700-1704.
ZHAO Hong, WEI Yong. Mechanism governing the pyrolytic corrosion at the flue gas side of the waterwall in a coal-fired boiler and its influencing factors[J]. Power Engineering, 2002, 22(2): 1700-1704.
- [8] 赵虹,吴广君,凌柏林等. 锅炉水冷壁高温氧化试验的热分析动力学研究[J]. 热能动力工程, 2005, 20(4): 397-401.
ZHAO Hong, WU Guang-jun, LING Bo-lin et al. Dynamic study of the thermal analysis of a water-wall high-temperature oxidation test in a boiler[J]. Engineering for Thermal Energy and Power, 2005, 20(4): 397-401.
- [9] 李景平,周年光,霍金仙等. 高温炉水中 Cl^- 对碳钢水冷壁管的腐蚀行为研究[J]. 材料保护, 2001, 34(8): 21-22.
LI Jing-ping, ZHOU Nian-guang, HUO Jin-xian et al. Study of the corrosion behavior of Cl^- in high-temperature boiler water on carbon steel waterwall tubes[J]. Material Protection, 2001, 34(8): 21-22.
- [10] Ernst P, Newman R C. Pit growth studies in stainless steel foils. II. Effect of temperature, chloride concentration and sulphate addition[J]. Corrosion Science, 2002, 44: 943-954.
- [11] Abd El Meguid E A, Abd El Latif A A. Electrochemical and SEM study on type 254 SMO stainless steel in chloride solutions[J]. Corrosion Science, 2004, 46: 2431-2444.

(陈滨 编辑)



150℃ 固化耐高温胶粘剂

本项目研制了一种 150℃ 固化耐高温无机胶粘剂,该胶粘剂以磷酸二氢铝为主体树脂,以氧化铝等金属氧化物为固化剂,该无机胶粘剂具有良好的耐久性能。150℃ 固化后最高使用温度可以达到 1000℃。目前已在俄罗斯、白俄罗斯等国家用于耐高温材料的粘接。

(如有需要者,请与编辑部联系)

used in tangentially-fired boilers. **Key words:** utility boiler on-line monitoring system acoustic wave method , aerodynamic field , industrial application

基于智能积分的电站锅炉主汽温 PID 控制 = **Main Steam Temperature PID Control of an Utility Boiler Based on the Intelligent Integration** [刊 汉] LI Jing-jing , ZHANG Xiao-dong , YAN Shui-bao (College of Chemical Industry and Energy Source , Zhengzhou University , Zhengzhou , China , Post Code: 450001) , ZHAO Rui-ju (Henan Electric Power Experiment Research Institute , Zhengzhou , China , Post Code: 450052) // Journal of Engineering for Thermal Energy & Power. -2012 27(1) . -86 ~90

Analyzed was the relationship between the PID control algorithm and the mathematical model for thermotechnical controlled objects and pointed out were that abundant information about the thermotechnical objects is contained in the errors and derivative results. To strengthen the analysis of the foregoing information can enhance the performance of the PID controllers. The transient process of a closed loop system under a stepped disturbance can be divided into two stages: the first stage is a non-balanced stationary state away from the balance state in thermodynamics. In a relatively long time period ,the CFB boiler , flying ash , nitrogen isothermal adsorption , pore structure intrinsic frequency will maintain its high order oscillation. The second stage is that the closed loop system enters into its linear non-balanced thermodynamic range. In such a case ,the PID controllers will be degraded to integral ones. With the free energy dissipation rate of the system serving as a parameter , a PID control algorithm was proposed based on an intelligent integration. The algorithm can transiently change the proportional gain and integration action ,and effectively enhance the speediness and stability of the system. A simulation test of the main steam object of a boiler indicates that the performance of the control algorithm is superior to that of conventional PID controllers. **Key words:** thermotechnical automatic control , intelligent integration , PID control , boiler , main steam temperature

锅炉水冷壁管在含 SO_4^{2-} 溶液中的点蚀特性研究 = **Study of the Pitting Characteristics of Boiler Water-wall Tube in SO_4^{2-} -contained Solution** [刊 汉] XIONG Shu-hua , ZHU Zhi-ping , JING Ling-ling , ZHANG Hui (College of Chemical and Biological Engineering , Changsha University of Science and Technology , Changsha , China , Post Code: 410076) // Journal of Engineering for Thermal Energy & Power. -2012 27(1) . -91 ~95

To study the pitting characteristics of waterwall tube material 15CrMo in SO_4^{2-} -contained solution , through a normal temperature electrochemical test and a high temperature plate-hanging test , an analysis was performed of the normal temperature performance and high temperature corrosion characteristics of the material in question. By using a lens reflection-based metallogenic microscope SEM ,EDS and XRD ,the morphology and constituents of the surface of the test piece were represented and analyzed. The research results show that at a normal temperature ,the oxidation

action of SO_4^{2-} will mainly dominates to contain the corrosion to the stainless steel ,thus enhancing the corrosion-resistant property of the material. At a high temperature SO_4^{2-} will become corrosive ions to quicken the pitting of the material ,thus forming pittings with serrated rims ,of which the critical pitting concentration will be 1 mg/L. At a normal temperature ,the mechanism to contain the Cl^- pitting by SO_4^{2-} lies in its competitive adsorption while at a high temperature ,the mechanism to promote the pitting by SO_4^{2-} lies in its local acidification theory. **Key words:** waterwall tube ,15CrMo SO_4^{2-} pitting

电厂用阳离子交换树脂高温分解特性研究 = **Study of the Pyrolytic Characteristics of Power-plant-purposed Cation Exchange Resin** [刊,汉] JING Ling-ling , ZHU Zhi-ping , ZHANG Hui , XIONG Shu-hua (College of Chemical and Biological Engineering , Changsha University of Science and Technology , Changsha , China , Post Code: 410076) // Journal of Engineering for Thermal Energy & Power. -2012 27(1) . -96 ~ 100

The pyrolysis by SO_4^{2-} leaked into a thermal system to break up cation resin represents one of the causes that the SO_4^{2-} content in a water-steam system of a power plant exceeds the standard. To solve such a problem ,the authors have studied the SO_4^{2-} pyrolysis characteristics of the commonly-used cation resin polished by condensate water in an autoclave. The research results show that after a pyrolysis of the cation resin ,its exchange functional group ($-\text{SO}_3\text{H}$) will fall off from the resin skeleton and produce a great quantity of acidic substances. The quantity of SO_4^{2-} produced by the pyrolysis will increase with the pyrolytic temperature and a surge phenomenon will emerge after the temperature exceeds 200 °C. The quantity of SO_4^{2-} produced by the old resin will be slightly less than that produced by the new resin ,however ,more acidic substances will be generated. At 280 °C ,the quantity of SO_4^{2-} produced by the cation resin will increase with an elapse of time. Both actually measured SO_4^{2-} and the result obtained from the infrared spectrum show that a certain quantity of resin is almost completely decomposed after 24 hours. **Key words:** cation exchange resin ,pyrolysis SO_4^{2-} ,ion chromatography ,infrared spectrum

海水脱硫散堆填料塔流体流动及传热研究 = **Study of the Fluid Flow and Heat Transfer in a Seawater Desulfurization Bulk Packing Tower** [刊,汉] GAO Mei-shan , WANG Shi-he (College of Civil Works , Southeast University , Nanjing , China , Post Code: 210096) , WANG Xiao-ming (Guodian Environmental Protection Research Institute , Nanjing , China , Post Code: 210013) , GUO Ming-chun (Shanghai Huolin Chemical Equipment Engineering Co. Ltd. , Shanghai , China , Post Code: 200127) // Journal of Engineering for Thermal Energy & Power. -2012 27(1) . -101 ~ 106

On a large-sized movable type seawater desulfurization test rig , a pilot-scale test was performed. On the basis of the volumetric average method , in combination with the pressure loss fitting formula obtained from the test data , a mod-